Received: 10 April 2022 | Revised: 4 June 2022 | Accepted: 1 July 2022

DOI: 10.1111/1462-2920.16124

RESEARCH ARTICLE

environmental microbiology Applied Microbiology International

Wide distribution of the *sad* gene cluster for sub-terminal oxidation in alkane utilizers

Chao-Fan Yin | **Ying Xu** | **Tao Li** | **Ning-Yi Zhou**

State Key Laboratory of Microbial Metabolism, Joint International Research Laboratory of Metabolic & Developmental Sciences, and School of Life Sciences & Biotechnology, Shanghai Jiao Tong University, Shanghai, China

Correspondence
Ning-Yi Zhou, Shanghai Jiao Tong University, 800 Dongchuan Road, Shanghai 200240, China.
Email: ningyi.zhou@sjtu.edu.cn

Funding information
National Key R&D Program of China, Grant/Award Number: 2021YFA0910300; National Natural Science Foundation of China, Grant/Award Number: 92051104

Abstract

Alkane constitutes major fractions of crude oils, and its microbial aerobic degradation dominantly follows the terminal oxidation and the sub-terminal pathways. However, the latter one received much less attention, especially since the related genes were yet to be fully defined. Here, we isolated a bacterium designated *Acinetobacter* sp. strain NyZ410, capable of growing on alkanes with a range of chain lengths and derived sub-terminal oxidation products. From its genome, a secondary alcohol degradation gene cluster (*sad*) was identified to be likely involved in converting the aliphatic secondary alcohols (the sub-terminal oxidation products of alkanes) to the corresponding primary alcohols by removing two-carbon unit. On this cluster, *sadC* encoded an alcohol dehydrogenase converting the aliphatic secondary alcohols to the corresponding ketones; *sadD* encoded a Baeyer–Villiger monooxygenase catalysing the conversion of the aliphatic ketones to the corresponding esters; SadA and SadB are two esterases hydrolyzing aliphatic esters to the primary alcohols and acetic acids. Bioinformatics analyses indicated that the *sad* cluster was widely distributed in the genomes of probable alkane degraders, apparently coexisting (64%) with the signature enzymes AlkM and AlmA for alkane terminal oxidation in 350 bacterial genomes. It suggests that the alkane sub-terminal oxidation may be more ubiquitous than previously thought.

INTRODUCTION

Alkane metabolism is an important part of the global carbon cycle (Austin & Groves, 2011), and bacteria play an extremely significant role in the remediation of crude oil-contaminated land and marine environments (Dell' Anno et al., 2021; Kiamarsi et al., 2019). It has hitherto remained a significant attention of researchers (Rojo, 2009; Rojo, 2010; Wentzel et al., 2007) and so far various microorganisms have been reported to have the ability to degrade alkanes (Wentzel et al., 2007).

Four alkane degradation pathways including terminal, sub-terminal, bi-terminal oxidation and Finnerty pathway have been postulated (Ji et al., 2013). However, the former two pathways (Rojo, 2010) were dominantly found among the alkane degraders (Figure 1) and the terminal oxidation pathway has been particularly well studied, including the genes encoding alkane terminal monooxygenases. AlkB characterized in great detail from *Pseudomonas putida* GPo1 is an integral-membrane non-heme diiron monooxygenase, requiring two electron transfer proteins rubredoxin and rubredoxin reductase (Nie et al., 2014; Van Beilen et al., 1994). Another similar system containing AlkM as the monooxygenase component was characterized from *Acinetobacter* sp. strain ADP1 (Ratajczak et al., 1998). Whereas AlmA from *Acinetobacter* sp. strain DSM 17874 is a single component FAD-dependent monooxygenase required for long-chain (C32 and C36) alkane degradation (Throne-Holst et al., 2007). An FMN-dependent two-component long-chain alkane (up to C36) monooxygenase LadA was also characterized from a Gram-positive *Geobacillus thermodenitrificans* strain NG80-2 (Feng et al., 2007; Li et al., 2008). In general, the terminal oxidation pathway catalysed by aforementioned monooxygenases begins with the hydroxylation of the terminal carbon atom of

© 2022 Society for Applied Microbiology and John Wiley & Sons Ltd.

14622920, 2022, 12, Downloaded from https://sfamjournals.onlinelibrary.wiley.com/doi/10.1111/1462-2920.16124 by Shanghai Jiao Tong University, Wiley Online Library on [19/12/2022]. See the Terms and Conditions (https://onlinelibrary.wiley.com/terms-and-conditions) on Wiley Online Library for rules of use; OA articles are governed by the applicable Creative Commons License

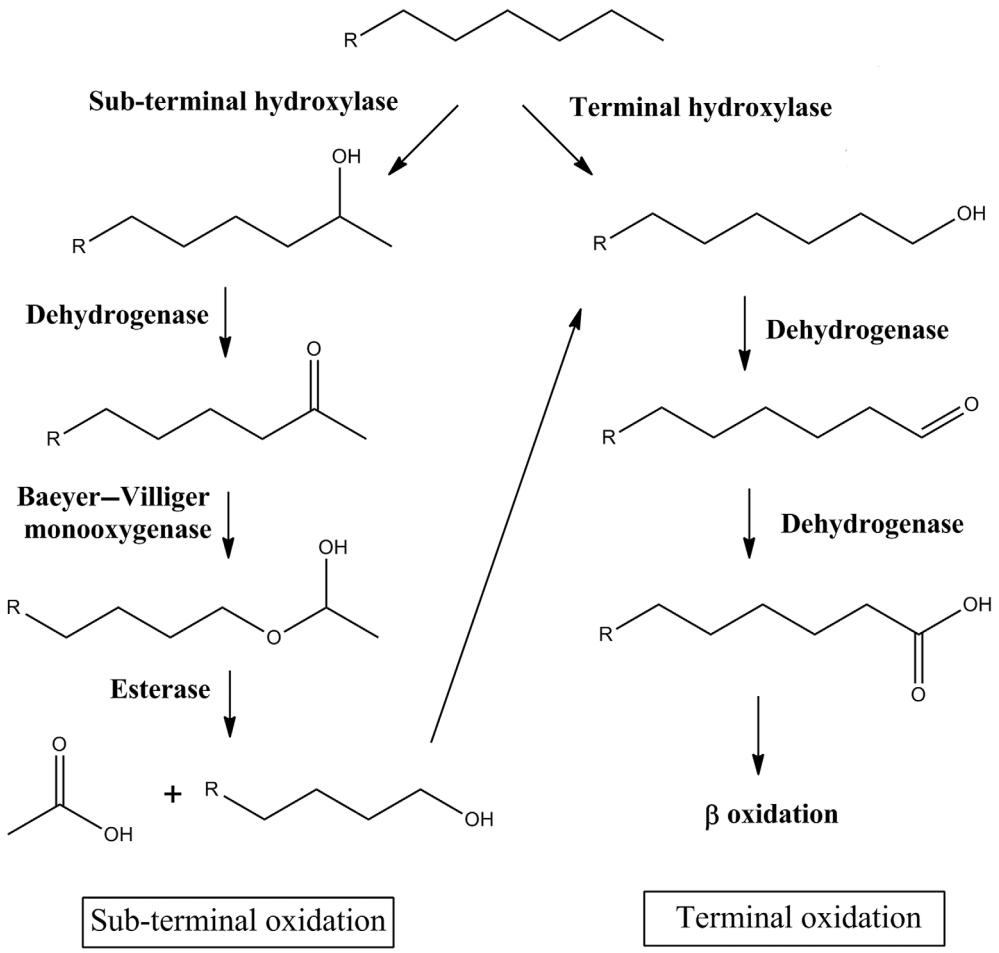

FIGURE 1 Two prototypical aerobic degradation pathways of alkanes

alkanes to form primary alcohols, followed by their conversion to the corresponding terminal carboxylic acids and then enter the conventional β-oxidation pathway. In contrast, studies on the sub-terminal degradation pathway are relatively scarce. This pathway starting with the hydroxylation of the sub-terminal carbon atom was proposed via a putative monooxygenase, converting the alkanes to the corresponding secondary alcohols, and followed by a dehydrogenase converting them into the corresponding ketone-containing compounds. A Baeyer–Villiger monooxygenase (BVMO) was proposed to inset an oxygen atom into the ketone-adjacent carbon–carbon bond to form the corresponding esters, which were finally cut by an esterase to form a shorter chain primary alcohol (Forney & Markovetz, 1970; Rojo, 2009). Although this sub-terminal oxidation pathway was proposed based on the detection of alkane degradation intermediates half century ago (Forney & Markovetz, 1970), the reports on their genetic determinants and biochemical evidence are very limited, except a rare gene cluster from *Pseudomonas fluorescens* strain DSM 50106 was biochemically proven to be capable of converting the aliphatic secondary alcohols to the corresponding primary alcohols (Kirschner et al., 2007a). However, this strain was incapable of growing on alkanes as well as their derived sub-terminal oxidation compounds (Kirschner et al., 2007a).

Here, we report the isolation of a bacterial strain capable of utilizing alkanes and the derived sub-terminal oxidation products for its growth. A gene cluster consisting of four genes was identified to encode enzymes involved in this oxidative pathway. Further bioinformatics analysis indicated a wide distribution of this cluster in the genomes of probable alkane degraders, suggesting the universal presence of this long-time overlooked sub-terminal degradation pathway in the alkane degraders.

EXPERIMENTAL PROCEDURES

Bacterial strains, plasmids, growth conditions and chemicals

All bacterial strains, plasmids and primers used in this study were listed in Table 1. *Acinetobacter* sp. strain NyZ410 was isolated from the gut of *Tenebrio molitor* larvae for the degradation of low-molecular-weight polyethylene.

14622920, 2022, 12, Downloaded from https://sfamjournals.onlinelibrary.wiley.com/doi/10.1111/1462-2920.16124 by Shanghai Jiao Tong University, Wiley Online Library on [19/12/2022]. See the Terms and Conditions (https://onlinelibrary.wiley.com/terms-and-conditions) on Wiley Online Library for rules of use; OA articles are governed by the applicable Creative Commons License

TABLE 1 Bacterial strains, plasmids and primers used in this study

Bacterial strains, plasmids or primers	Descriptions or sequences (5′ to 3′)	Sources or references
Bacterial strains		
E. coli DH5a	*lacU169ΔlacU169 (φ80dlacZΔM15) hsdR17 recA1 endA1 hsdR17 thi*$^{-1}$ *gyrA96 relA1*	Novagen
E. coli BL21(DE3)	F$^-$ *ompT hsdS*$_B$ *(Rb*$^-$*mB*$^-$*) gal (λcI857 ind1 Sam7 nin5 lac*UV5-T7gene1*) dcm* (DE3)	Novagen
Acinetobacter sp. strain NyZ410	Wild type, capable of growing on alkanes and derived aliphatic secondary alcohols/ketones	This study
Plasmids		
pET-28a(+)	Km^r, overexpression vector	Novagen
pETDuet-1	Amp^r, co-expression vector	Novagen
pET-28a-*sadC*	*sadC* cloned into pET-28a(+)	This study
pET-28a-*sadD*	*sadD* cloned into pET-28a(+)	This study
pET-28a-*sadA*	*sadA* cloned into pET-28a(+)	This study
pET-28a-*sadB*	*sadB* cloned into pET-28a(+)	This study
pETDuet-*sad*	*sad* cluster cloned into pETDuet-1	This study
Primers		
*sadD*_F	GTGCCGCGCGGCAGCCATATGATGACAACAGAAACAACTTTAGCTACG	Forward primer for *sadD*
*sadD*_R	ACGGAGCTCGAATTCGGATCCTTATTTTTTACTCACGCTATAATGGTTTA	Reverse primer for *sadD*
*sadC*_F	GTGCCGCGCGGCAGCCATATGATGGATTTAAAGTTTATGGGTATTTTTT	Forward primer for *sadC*
*sadC*_R	ACGGAGCTCGAATTCGGATCCTTATTTGATGTATTTGTTAAATAATGGATATC	Reverse primer for *sadC*
*sadA*_F	GTGCCGCGCGGCAGCCATATGATGTTCGCTAAGCCAATTAAGAAA	Forward primer for *sadA*
*sadA*_R	ACGGAGCTCGAATTCGGATCCTTATGAACGCAATGCAGGATAAA	Reverse primer for *sadA*
*sadB*_F	GTGCCGCGCGGCAGCCATATGATGTTACTTGCTAAGCCTGTCAAAA	Forward primer for *sadB*
*sadB*_R	ACGGAGCTCGAATTCGGATCCTTACATCCGTAAAGCAGGGGTAA	Reverse primer for *sadB*
Duet (*sadC_sadD*)_F	TCATCACCACAGCCAGGATCCGATGGATTTAAAGTTTATGGGTATTTTTT	Forward primer for fragment of *sadC* and *sadD*
Duet (*sadC_sadD*)_R	GCATTATGCGGCCGCAAGCTTTTATTTTTTACTCACGCTATAATGGTTTA	Reverse primer for fragment of *sadC* and *sadD*
Duet (*sadA_sadB*)_F	TAAGAAGGAGATATACATATGATGTTACTTGCTAAGCCTGTCAAAA	Forward primer for fragment of *sadA* and *sadB*
Duet (*sadA_sadB*)_R	TTTACCAGACTCGAGGGTACCTTATGAACGCAATGCAGGATAAA	Reverse primer for fragment of *sadA* and *sadB*

The strain was cultivated at 30°C with a liquid carbon-free basal medium (LCFBM) as previously reported (Yang et al., 2014). Alkanes (including hexadecane, eicosane, triacontane, etc.) and derived sub-terminal oxidation compounds (including 2-tetradecanol, 2-hexadecanone, 3-tetradecanone and 9-heptadecanone) were added in LCFBM (1%, wt./vol.) served as carbon sources. *Escherichia coli* was grown on lysogeny broth (LB) (Sambrook et al., 1989) at 37°C with kanamycin (50 μg/ml) or ampicillin (100 μg/ml) based on experimental requirements. All the alkanes and derived sub-terminal oxidation compounds were purchased from Sigma (St. Louis, MO, USA) or Aladdin Reagent Co. Ltd. (Shanghai, China).

Genome and transcriptome sequencing

Genome sequencing of strain NyZ410 was conducted using a PacBio RS II platform and Illumina HiSeq 4000 platform in the Beijing Genomics Institute (BGI, Shenzhen, China). The complete genome has been deposited in GenBank (accession number: CP094620). For transcriptome sequencing, strain NyZ410 was cultured with sodium succinate and then treated by sodium succinate and polyethylene with a concentration of 0.5% (wt./vol.). RNA sequencing was accomplished using the Illumina HiSeq 4000 platform in the Beijing Genomics Institute (BGI). The RNA seq data have been deposited in SRA (BioProject accession number: PRJNA820384).

Gene cloning, protein overexpression and purification

The genes *sadA*, *sadB*, *sadC* and *sadD* were PCR-amplified from the genome of strain NyZ410 with primers listed in Table 1 respectively and then fused

14622920, 2022, 12, Downloaded from https://sfamjournals.onlinelibrary.wiley.com/doi/10.1111/1462-2920.16124 by Shanghai Jiao Tong University, Wiley Online Library on [19/12/2022]. See the Terms and Conditions (https://onlinelibrary.wiley.com/terms-and-conditions) on Wiley Online Library for rules of use; OA articles are governed by the applicable Creative Commons License

into pET-28a(+) (digested with NdeI and BamHI) to yield N-terminal His_6-tagged protein overexpression constructs pET-28a(+)-*sadD*, pET-28a(+)-*sadC*, pET-28a(+)-*sadA* and pET-28a(+)-*sadB* using a One Step cloning kit (Vazyme Biotech Co., Ltd.). The sequence-validated constructs were transformed into *E. coli* BL21 (DE3) by a standard procedure (Sambrook et al., 1989). The generated recombinant strains BL21(DE3) [pET-28a(+)-*sadD*], BL21(DE3)[pET-28a(+)-*sadC*], BL21(DE3)[pET-28a(+)-*sadA*] and BL21(DE3)[pET-28a(+)-*sadB*] were cultivated on LB with kanamycin (50 μg/ml) at 180 rpm and 37°C until an OD_{600} of 0.6, then induced with 0.1 mM IPTG at 150 rpm and 16°C overnight for 16 h.

The harvested cells were used to conduct ultrasonic fragmentation after being washed and resuspended with PB buffer [100 mM, pH 7.4; 200 mM NaCl, 10% (vol./vol.) glycerol]. The cell extracts were obtained through centrifugation at 13,000*g* at 4°C for 40 min and then filtered with 0.45 μm filter membranes. Protein purification was conducted using the ÄKTA start system (GE Healthcare) equipped with a 5-ml HisTrap HP column (GE Healthcare). The column was washed with 20 mM imidazole dissolved in PB buffer, the bound protein was eluted by increasing imidazole concentration to 250 mM, and residual imidazole was then removed from the protein solution through an ultrafiltration tube. The resulting recombinant His_6-tagged proteins were assessed by SDS-PAGE, and the concentration was determined by spectrophotometry at 280 nm (Kielkopf et al., 2020) using a Nano-300 spectrophotometer (Allsheng Instruments Co., Ltd., Hangzhou, China).

Enzyme activity assay

To test the enzymatic activity of SadD, keto-containing alkanes (1 mM each), NADPH (1 mM), FAD (0.02 mM) and SadD (1 mg) were all added into PB buffer [100 mM, pH 7.4; 200 mM NaCl, 10% (vol./vol.) glycerol] and the reaction was carried out for 2 h at 30°C. After the reaction, an equal volume of *n*-hexane was added for extraction and the product was identified by GC–MS analysis. Same reaction system without enzyme served as a control.

Proteins SadC, SadA and SadB formed inclusion bodies when expressed in *E. coli*; their activity assay was then conducted using crude cell extracts instead. During SadC activity assay, substrates cyclohexanone, 2-tetradecanol and 2-tetradecanone (0.2%, vol./vol. each) were added to 500 μl of crude cell extracts (approximately 20 mg/ml) and the reaction was conducted at 37°C for 2 h. At the end of the reaction, an equal volume of *n*-hexane was added for extraction, and the substrate was then derivatized with trimethylsilane before GC–MS analysis. Crude extracts of *E. coli* cells containing pET-28a(+) vector served as the control.

The proteins SadA and SadB were bioinformatically predicted as membrane proteins containing apparent transmembrane regions. They were likely combined with cell debris, which was also shown by SDS-PAGE analysis. Therefore, the enzymatic activity assay for SadA and SadB was conducted using the cell debris as no activity was detected from the cell extracts of recombinant *E. coli*. In this test, dodecyl acetate served as the substrate, the cell debris and substrate were both added into 500 μl PB buffer. After the reaction, the sample was prepared as above and analysed by GC–MS. *Escherichia coli* cell debris containing pET-28a(+) vector served as a control.

Construction of pETDuet-*sad* and whole-cell biotransformation of 2-tetradecanol

To construct the coexpression vector of pETDuet-*sad*, the gene fragment containing both *sadD* and *sadC* was amplified and inserted into MCS1 of pETDuet-1 using One Step cloning kit (Vazyme Biotech Co., Ltd.) to yield pETDuet-*sadD_sadC*. Subsequently, the fragment containing both *sadA* and *sadB* were then inserted to MCS2 of pETDuet-*sadD_sadC* to yield pETDuet-*sad* with the same method. The sequence-validated coexpression plasmids were then transformed into *E. coli* BL21 (DE3).

Recombinant cells *E. coli* BL21 (DE3) [pETDuet-*sad*] and *E. coli* BL21 (DE3) [pETDuet] were cultivated and induced as previously mentioned. After being washed and resuspended in PB buffer (100 mM, pH 7.4) with a final OD_{600} of 15, 2-tetradecanol was added with a concentration of 2 mg/ml and the biotransformation was conducted at 30°C, 180 rpm for 24 h. The samples collected at the appropriate time were analysed by GC–MS after the aforementioned extraction and derivatization.

GC-MS analysis

Compounds analysis was performed with a GC–MS system (Agilent, USA) consisting of 7890B-GC equipped with an HP-5MS separation column (30 cm × 0.25 mm × 0.25 μm) and 5977B-MS detector. The carrier gas (helium) was supplied at 1 ml/min. A volume of 1 μl was injected with a splitless mode. The temperatures of injector, transfer line and MS source were set at 280°C, 290°C and 230°C respectively. The oven temperature program was started at 70°C (2 min) and increased at 5°C/min to 130°C and at 10°C/min to 180°C then at 5°C/min to 285°C (1 min). The MS detector used 70 eV for ionization. The identification of peaks was performed by comparing the retention times with those of authentic compounds, and mass spectra to the profiles in NIST database.

14622920, 2022, 12, Downloaded from https://sfamjournals.onlinelibrary.wiley.com/doi/10.1111/1462-2920.16124 by Shanghai Jiao Tong University, Wiley Online Library on [19/12/2022]. See the Terms and Conditions (https://onlinelibrary.wiley.com/terms-and-conditions) on Wiley Online Library for rules of use; OA articles are governed by the applicable Creative Commons License

Bioinformatics analysis

Distribution of *sad* cluster

All publically available bacterial genomes (including the genomes of typical alkane-degrading bacteria) in NCBI GenBank (up to July 2021) were queried via MultiGeneBlast (Medema et al., 2013a) with default parameters to identity target homologous *sad* clusters. Taxonomic distribution and composition of the retrieved significant hits (sequence identity >30%) of target gene cluster were calculated and visualized by Origin 85.

Coexistence of SadD with alkane-degrading signature enzymes AlmA/AlkM

AlmA, AlkM and the SadD characterized in this study were queried in bacterial genomes separately via BLASTP (sequence identity >60%), and Venn analysis was conducted on the list of bacteria containing the query proteins.

Phylogenetic analysis of the Baeyer–Villiger monooxygenase homologues from reviewed protein sequences database

Homologues search of SadD characterized in this study was performed using BLASTP against the UniRef90 protein database (up to January of 2022), and a total of 1756 homologues were selected with over 40% identity and at least 70% coverage. These sequences as well as SadD were aligned by MUSCLE v5.1 (Edgar, 2021) and then used to construct profile Hidden Markov Model (pHMM) with hmmbuild program from the HMMER 3.0 package (Finn et al., 2011). The pHMM was then used to inspect protein sequences in UniProt/Swiss-Prot databases with hmmsearch program from the HMMER3.0 package. A total of 53 reviewed protein sequences with bit scores over 180 and two manually added BVMOs (BmoF1 from *Pseudomonas fluorescens* strain DSM 50106 (Kirschner et al., 2007b) and MekA from *Pseudomonas veronii* strain MEK700 (Volker et al., 2008), the UniProt entry names were O87636 and Q0MRG6 respectively) as well as SadD were aligned by MUSCLE v5.1 (Edgar, 2021). The best-fitting protein evolutionary models (LG + I + G4 + F) for the data set was selected by ModelTest-NG (Darriba et al., 2020) to construct the phylogenetic tree with bootstrap 1000 replicates using RAxML-NG (Stamatakis, 2014), which was then visualized and annotated by iTOL (Letunic & Bork, 2019).

Prediction of three-dimensional structure and molecular docking simulation

After protein structure of SadD was predicted by AlphaFold v2.0 (Jumper et al., 2021), its model was then aligned with other two prototypical BVMO protein structures (PDB code: 2YLT and 3UCL) and visualized using PyMOL (The PyMOL Molecular Graphics System, Version 2.5.2 Schrödinger, LLC) (Schrodinger, 2015).

Molecular docking of the 2-undecanone to SadD model was carried out using AutoDock4.2 (Morris et al., 2009), where non-polar H atoms were merged onto both the ligands and the targets using AutoDockTools prior to performing the docking. The best docking

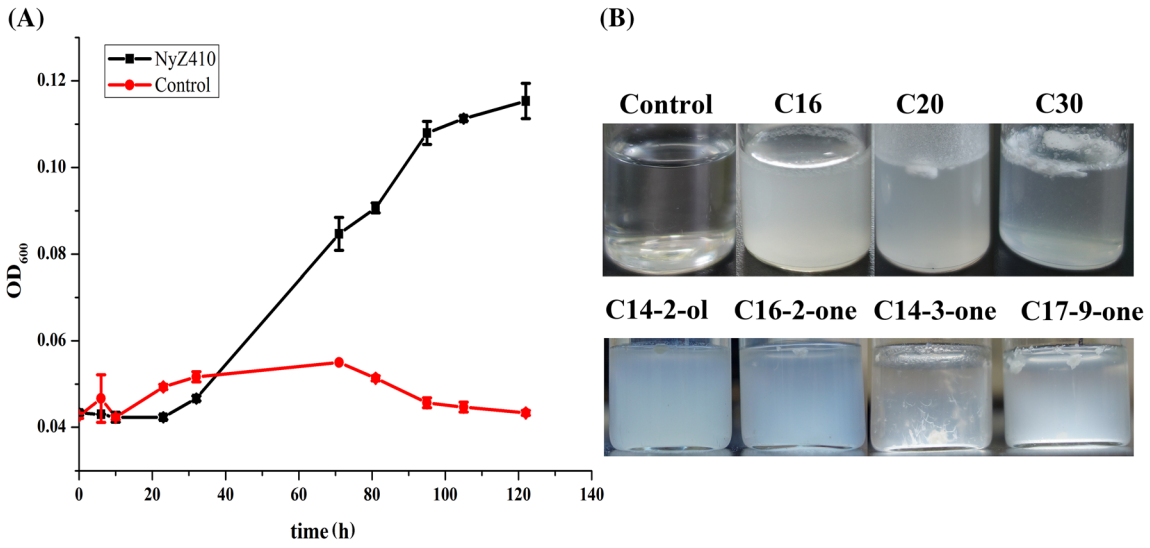

FIGURE 2 The growth of *Acinetobacter* sp. strain NyZ410 on alkanes and derived sub-terminal oxidation compounds. (A) Growth curve of the strain NyZ410 with 2-tetradecanol. (B) Growth of the strain NyZ410 indicated by turbidity in the culture on alkanes [hexadecane (C16), eicosane (C20), triacontane (C30)] and derived sub-terminal oxidation compounds [2-tetradecanol (C14-2-ol), 2-hexadecanone (C16-2-one), 3-tetradecanone (C14-3-one), and 9-heptadecanone (C17-9-one)]. The strain was cultivated in basal medium containing substrates (1%, wt./vol.) at 30°C, 180 rpm. The same system without inoculation served as a control

14622920, 2022, 12, Downloaded from https://sfamjournals.onlinelibrary.wiley.com/doi/10.1111/1462-2920.16124 by Shanghai Jiao Tong University, Wiley Online Library on [19/12/2022]. See the Terms and Conditions (https://onlinelibrary.wiley.com/terms-and-conditions) on Wiley Online Library for rules of use; OA articles are governed by the applicable Creative Commons License

model with the lowest binding energy (−4.07 kcal/mol) was selected.

RESULTS

Acinetobacter sp. strain NyZ410 was capable of growing on alkanes and their derived sub-terminal oxidation compounds

Acinetobacter sp. strain NyZ410 was isolated from the gut of *Tenebrio molitor* larvae for the degradation of low-molecular-weight polyethylene [The molecular weight ranges from approximately 100 to 10,000 Da (C10 to C700) determined by gel permeation chromatography]. In addition, it is also capable of utilizing alkanes with different lengths of chain (up to C36) as well as their derived alkane sub-terminal oxidation substrates (2-tetradecanol as well as 3-tetradecanone, 2-hexadecanone, 9-heptadecanone, etc.) for its growth (Figure 2). This suggested that the sub-terminal oxidation pathway is involved in alkane degradation by strain NyZ410.

Location of key genes involved in the conversion of secondary alcohol

Transcriptome analysis showed that some putative genes related to alkane degradation were upregulated when the strain NyZ410 was induced by low-molecular-weight polyethylene. Of them, putative alkane terminal hydroxylases including AlkM and AlmA homologues share 78% and 82% sequence identities with their functionally identified counterparts (GenBank accession numbers are O31250.1 and Q6F7T9.1) from *Acinetobacter baylyi* strain ADP1, respectively. Further analysis also showed an upregulated gene cluster [designated *sad* (**s**econdary **a**lcohol **d**egradation) cluster], consisting of four genes (*sadA*, *sadB*, *sadC* and *sadD*) likely involved in the alkane sub-terminal degradation [Figure 3(A)]. Among them, SadD shares a 43% amino acid sequence identity with a BVMO (GenBank accession number: Q9I3H5.1) from *Pseudomonas aeruginosa* PAO1, which converts the bicyclo[3.2.0]hept-2-en-6-one to the corresponding lactone. SadC shares a 38% sequence identity with a meso-2,3-butanediol dehydrogenase (GenBank accession number: Q48436.2) from *Klebsiella pneumoniae*, catalysing the reversible reduction of (*S*)-acetoin to 2,3-butanediol in the presence of NADH. Both SadA and SadB were annotated as metal-dependent hydrolases sharing a 59% sequence identity with each other but no evident sequence identity was found with other functionally characterized proteins. Based on this, an alkane sub-terminal degradation pathway [Figure 3(B)] catalysed by these enzymes was proposed in strain NyZ410 when their functions are established (see below).

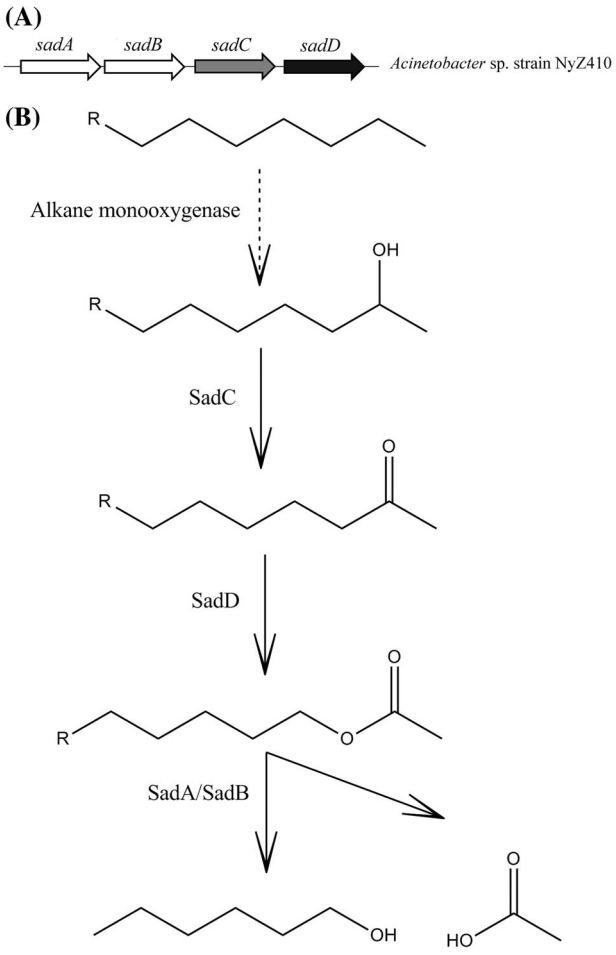

FIGURE 3 A proposed alkane degradation pathway catalysed by the aliphatic secondary alcohol degradation gene cluster (*sad*) encoded products in *Acinetobacter* sp. strain NyZ410. (A) Genomic organization of *sad* cluster. The arrows indicate the transcription direction of each gene. (B) Proposed alkane degradation pathway catalysed by *sad* encoded products. SadC: dehydrogenase; SadD: Baeyer–Villiger monooxygenase; SadA/SadB: esterases

Degradation of secondary alcohol with recombinant Sad enzymes in *E. coli*

To functionally characterize the four enzymes encoded by *sadABCD*, each gene was cloned into pET-28a(+) individually and heterologous expressed in *E. coli* BL21 (DE3). Unfortunately, except SadD, none of their products was successfully purified from the recombinant cells. Therefore, purified SadD and crude extracts of the other enzymes were used for enzymatic activity assay. As a model compound of aliphatic secondary alcohol, 2-tetradecanol (2-TDol, also a growth substrate for strain NyZ410 as shown in Figure 2) was selected for the assay. The GC–MS results revealed that SadC was a dehydrogenase capable of converting 2-tetradecanol to 2-tetradecanone [Figure 4(A,F)], SadD was a BVMO catalysing the conversion of 2-tetradecanone to dodecyl acetate [Figure 4(B,F)],

14622920, 2022, 12, Downloaded from https://sfamjournals.onlinelibrary.wiley.com/doi/10.1111/1462-2920.16124 by Shanghai Jiao Tong University, Wiley Online Library on [19/12/2022]. See the Terms and Conditions (https://onlinelibrary.wiley.com/terms-and-conditions) on Wiley Online Library for rules of use; OA articles are governed by the applicable Creative Commons License

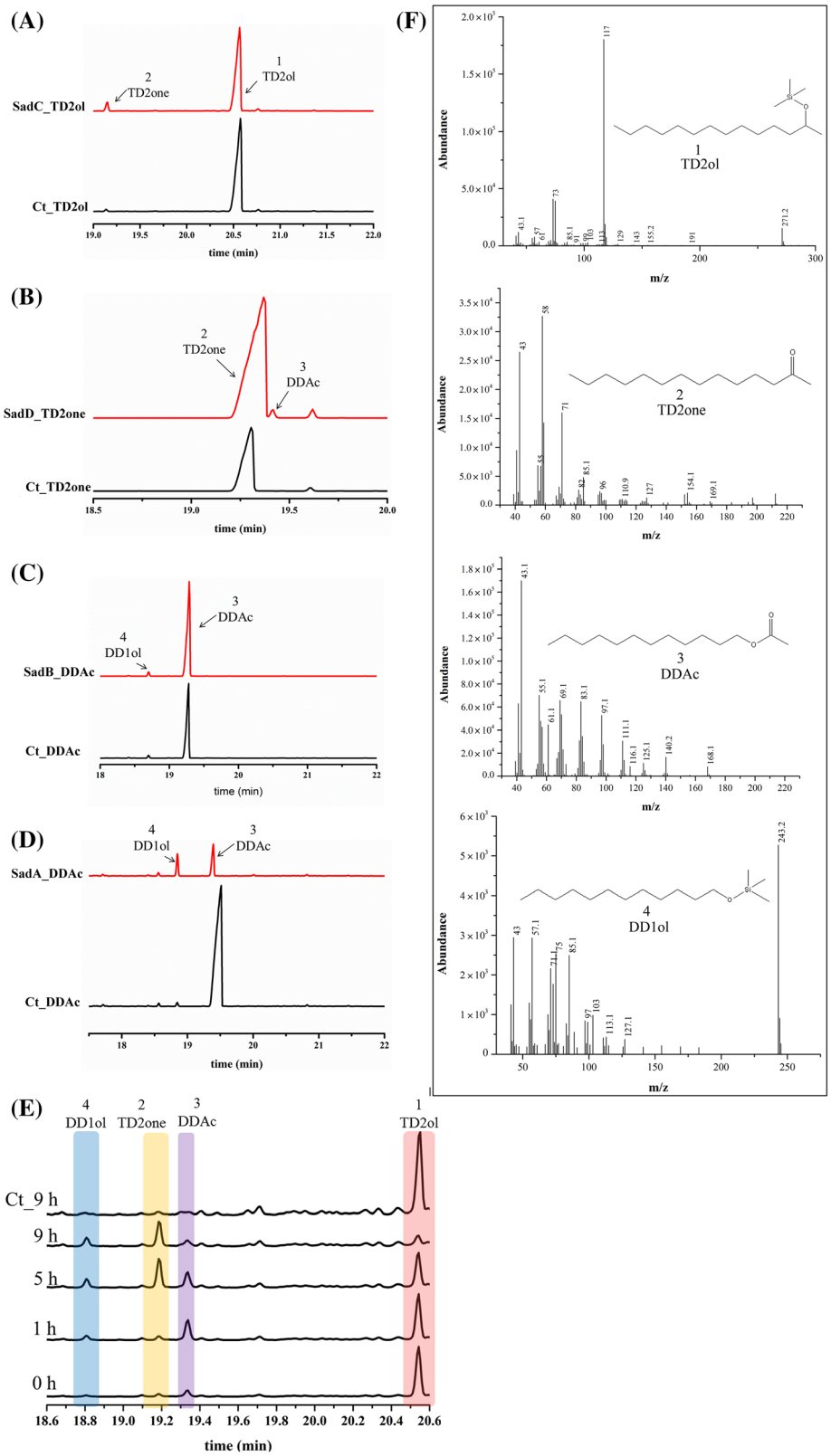

FIGURE 4 GC–MS analyses of the products from biochemical reactions catalysed by Sad enzymes in secondary alcohol degradation of alkane pathway. GC traces showing the conversion of 2-tetradecanol (TD2ol; compound 1) to 2-tetradecanone (TD2one; compound 2) by SadC (A). GC traces showing the conversion of 2-tetradecanone (TD2one; compound 2) to dodecyl acetate (DDAc; compound 3) by SadD (B). GC traces showing the conversions of dodecyl acetate (DDAc; compound 3) to 1-dodecanol (DD1ol; compound 4) by SadA (C) and SadB (D). GC trances showing the biotransformation of 2-tetradecanol (TD2ol) by recombinant *E. coli* BL21 (DE3) containing the entire *sad* cluster (E), where substrate 2-tetradecanol (TD2ol; compound 1) was converted to 1-dodecanol (DD1ol; compound 4) over time, with intermediates being 2-tetradecanone (TD2one; compound 3) and dodecyl acetate (DDAc; compound 4). MS spectra of the compounds 1–4 in above reactions (F)

14622920, 2022, 12, Downloaded from https://sfamjournals.onlinelibrary.wiley.com/doi/10.1111/1462-2920.16124 by Shanghai Jiao Tong University, Wiley Online Library on [19/12/2022]. See the Terms and Conditions (https://onlinelibrary.wiley.com/terms-and-conditions) on Wiley Online Library for rules of use; OA articles are governed by the applicable Creative Commons License

TABLE 2 Relative activities of SadD against different substrates

Substrates	Relative activity (%)[a]
2-Decanone	60
2-Tridecanone	74
2-Tetradecanone	100
2-Hexadecanone	74
3-Tetradecanone	ND
9-Heptadecanone	ND
2-Octadecanone	ND
Acetophenone	ND
Cyclohexanone	ND

ND: Not detected.
[a]This refers to activity relative to that on 2-tetradecanone (converting 0.22 μmol substrate using 1 mg protein for 2 h; set at 100) measured at 1 mM for each substrate in the same reaction conditions.

and SadA or SadB was responsible for the hydrolysis of dodecyl acetate to acetate and 1-dodecanol [Figure 4(C,D,F)]. Substrate specificity analysis revealed that SadD was active towards medium-chain aliphatic 2-keto (instead of 3-keto) compounds ranging from C10 to C16, and had the highest catalytic activity for 2-tetradecanone (Table 2).

In the verification of the function of *sad* in cascade reaction of the alkane degradation, the strain BL21 (DE3) [pETDuet-*sad*] containing entire *sad* cluster of four genes could progressively convert substrate 2-tetradecanol to 1-dodecanol, with both 2-tetradecanone and dodecyl acetate being also detected as intermediates in this process as shown in Figure 4(E,F). In principle, this recombinant strain should be able to grow on 2-tetradecanol because the acetate produced from 2-tetradecanol would support its growth. But it turned out that this strain had no ability to grow, probably due to the low transformation efficiency of *sad* encoded products.

Ubiquitous distribution of aliphatic secondary alcohol degradation gene clusters (*sad*) in genomes of probable alkane degraders

MulitiGeneBlast search (Medema et al., 2013b) was carried out to reveal possible presence of *sad* cluster in alkane degraders, using SadABCD sequence as the query. This search was performed against the available genomes of virtually all well-studied alkane degraders including *Acinetobacter baylyi* strain ADP1, *Pseudomonas aeruginosa* strain PAO1, *Pseudomonas protegens* strain CHA0, *Alcanivorax dieselolei* strain B5, *Alcanivorax borkumensis* strain SK2 and *Geobacillus thermodenitrificans* strain NG80-2. All these five degraders but strain NG80-2 contain a partial or complete gene cluster similar to *sad*, with *sadC* and *sadD* being always clustered together [Figure 5(A)]. To understand the distribution of the *sad* cluster in available bacterial genomes, its query file was further searched against all bacterial genomes in GenBank (up to July of 2021). The search results showed that homologous *sad*-encoded products were extremely enriched in many common alkane-degrading bacterial populations, including genera *Acinetobacter*, *Pseudomonas*, *Mycobacteroides*, *Rhodococcus*, *Mycobacterium*, *Nocardia*, *Alcanivorax*, *Marinobacter*, etc., as summarized in a review article (Wentzel et al., 2007) [Figure 5(C)]. This result gives a clue to the underlying physiological significance of the *sad* in the bacterial alkane degradation. For further verification of the genotype–phenotype correlation between the *sad* and alkane degradation, two prototypical alkane monooxygenase encoding genes *almA* (Throne-Holst et al., 2007) and *alkM* (Ratajczak et al., 1998) were selected as signatures for alkane degrading phenotype. The results by BLASTP search revealed that as much as 64% of bacteria (at least 26 strains from aquatic environments) contained all three genes among 350 bacterial genomes retrieved [Figure 5(B)]. It is worth mentioning that all of the alkane degradation phenotype-confirmed strains as shown in Figure 5(A) also contained *alkM* and *almA*. All of these results indicated that the *sad* cluster was broadly distributed in genomes of probable alkane-degrading bacteria and likely involved in alkane degradation.

Structure and substrate specificity of Baeyer–Villiger monooxygenases in alkane degradation

Most of the biochemically characterized BVMOs were promiscuous enzymes (Dudek et al., 2014), capable of catalysing more than one type of substrates. However, SadD in this study was active to aliphatic linear ketones but had no activity towards other types of ketones such as cyclohexanone (cyclic ketone) or acetophenone (aromatic ketones) (Table 2). To further understand the sequence–function relationship, the available reviewed protein sequences of homologues BVMO of SadD were retrieved from the database (UniProt/Swiss-Prot) to construct a phylogenetic tree, where the major type of substrates of the BVMOs was annotated (Figure 6). It was evident, to some extent, that BVMOs with the similar substrate specificity were clustered together. For example, BVMOs in clades IV, V, VI and VII catalysing the conversion of large macrocyclic compounds, typically used as intermediates in the biosynthesis of complex metabolites such as alkaloids and antibiotics, were clustered together; BVMOs in clade IV active towards small molecules, such as cyclohexanone (cyclic ketones), phenylacetone (aromatic ketones) and acetone (short-chain linear ketones), were clustered together. SadD was clustered together with BmoF1

14622920, 2022, 12, Downloaded from https://sfamjournals.onlinelibrary.wiley.com/doi/10.1111/1462-2920.16124 by Shanghai Jiao Tong University, Wiley Online Library on [19/12/2022]. See the Terms and Conditions (https://onlinelibrary.wiley.com/terms-and-conditions) on Wiley Online Library for rules of use; OA articles are governed by the applicable Creative Commons License

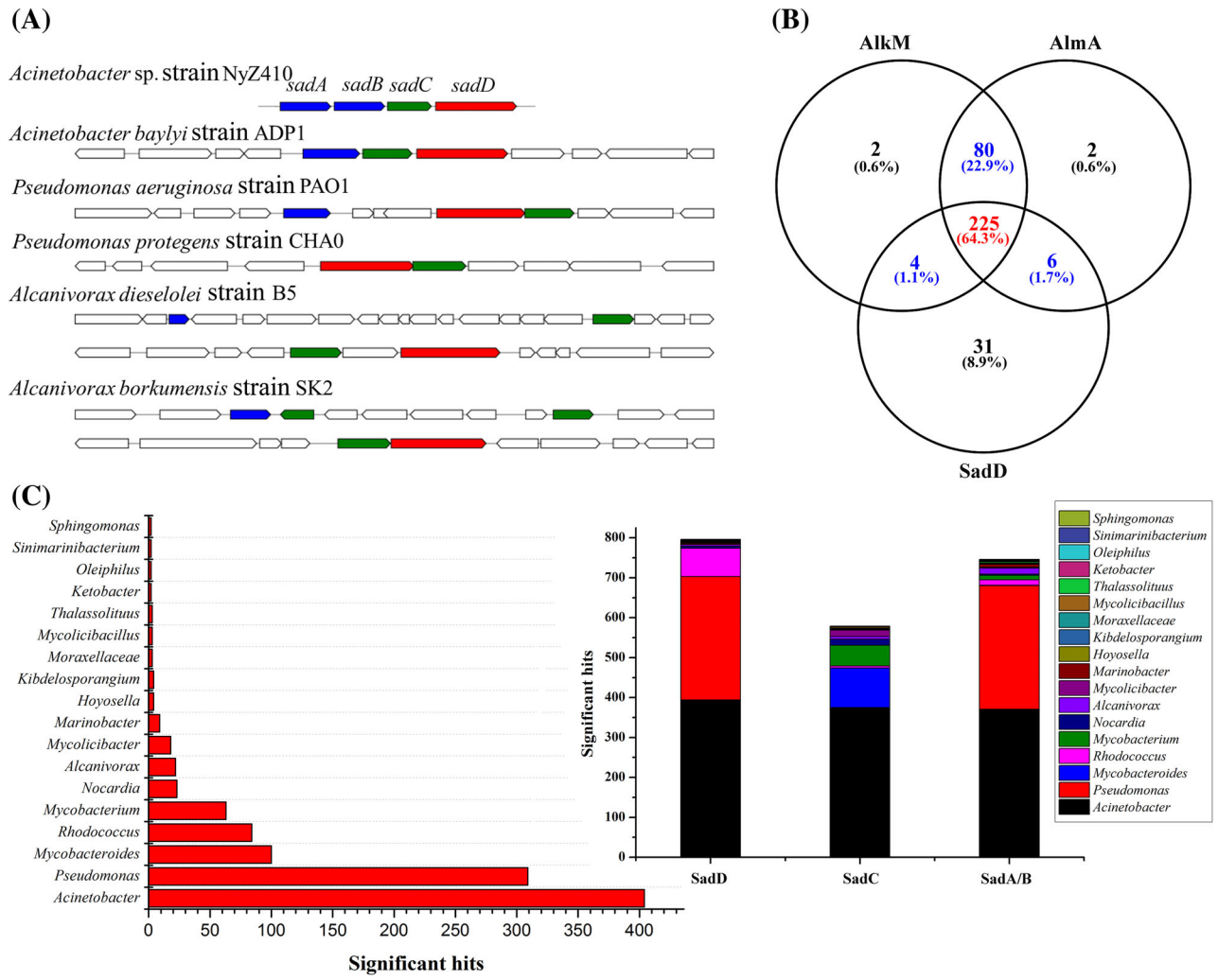

FIGURE 5 Wide distribution of the aliphatic secondary alcohol degradation gene cluster (*sad*) in the probable alkane degraders. (A) Distribution of the *sad* genes in genomes of typical alkane-degrading bacteria. Homologues proteins are indicated by identical colours. (B) Venn diagram shows that the Baeyer–Villiger monooxygenase SadD studied here apparently coexist with well-known alkane degradation signature enzymes AlmA (Throne-Holst et al., 2007) and AlkM (Ratajczak et al., 1998) in bacterial genomes. Each protein is deemed to be found in bacterial proteomes with the threshold of over 60% sequence identity. A total of 350 bacterial strains containing at least one of these three protein homologues were retrieved by BLASTP search as described in Experimental procedures. The numbers and the corresponding percentages of bacterial strains containing one, two and all of the three proteins are marked as black, blue and red respectively. (C) Taxonomic distribution (left panel) and composition analysis (right panel) of the *sad* in bacteria. Taxonomic distribution analysis of *sad* performed by MultiGeneBlast (Medema et al., 2013) revealed that *sad* enriched in common alkane-degrading species from *Acinetobacter*, *Pseudomonas*, *Mycobacteroides*, *Rhodococcus*, *Mycobacterium*, *Nocardia*, *Alcanivorax*, *Marinobacter*, and so on. Composition analysis of the significant hits revealed that the *sad* cluster was mostly abundant in *Acinetobacter* spp., and *sadD* was most conserved in the *sad* gene clusters

(UniProt entry: O87636) in clade I, which is the only other studied BVMO active to medium-chain aliphatic ketones from *Pseudomonas fluorescens* strain DSM 50106 (Kirschner et al., 2007b). It is therefore reasonable to propose that the substrate preferences of BVMOs are likely determined by the shape (linear or cyclic) or size (length of linear aliphatic chain or size of the cyclic) of the substrates, which may coordinate the distinct substrate-binding pockets of different BVMOs, but stronger evidence are needed to justify this hypothesis.

DISCUSSION

In this study, we biochemically identified an aliphatic secondary alcohol degradation gene cluster *sadABCD* from *Acinetobacter* sp. strain NyZ410, which was broadly distributed in genomes of probable alkane degraders and closely related to alkane sub-terminal degradation through further bioinformatics analysis. This study gives us a clue to further understand the significance of the long-time overlooked sub-terminal degradation pathway in microbial alkane degradation.

14622920, 2022, 12, Downloaded from https://sfamjournals.onlinelibrary.wiley.com/doi/10.1111/1462-2920.16124 by Shanghai Jiao Tong University, Wiley Online Library on [19/12/2022]. See the Terms and Conditions (https://onlinelibrary.wiley.com/terms-and-conditions) on Wiley Online Library for rules of use; OA articles are governed by the applicable Creative Commons License

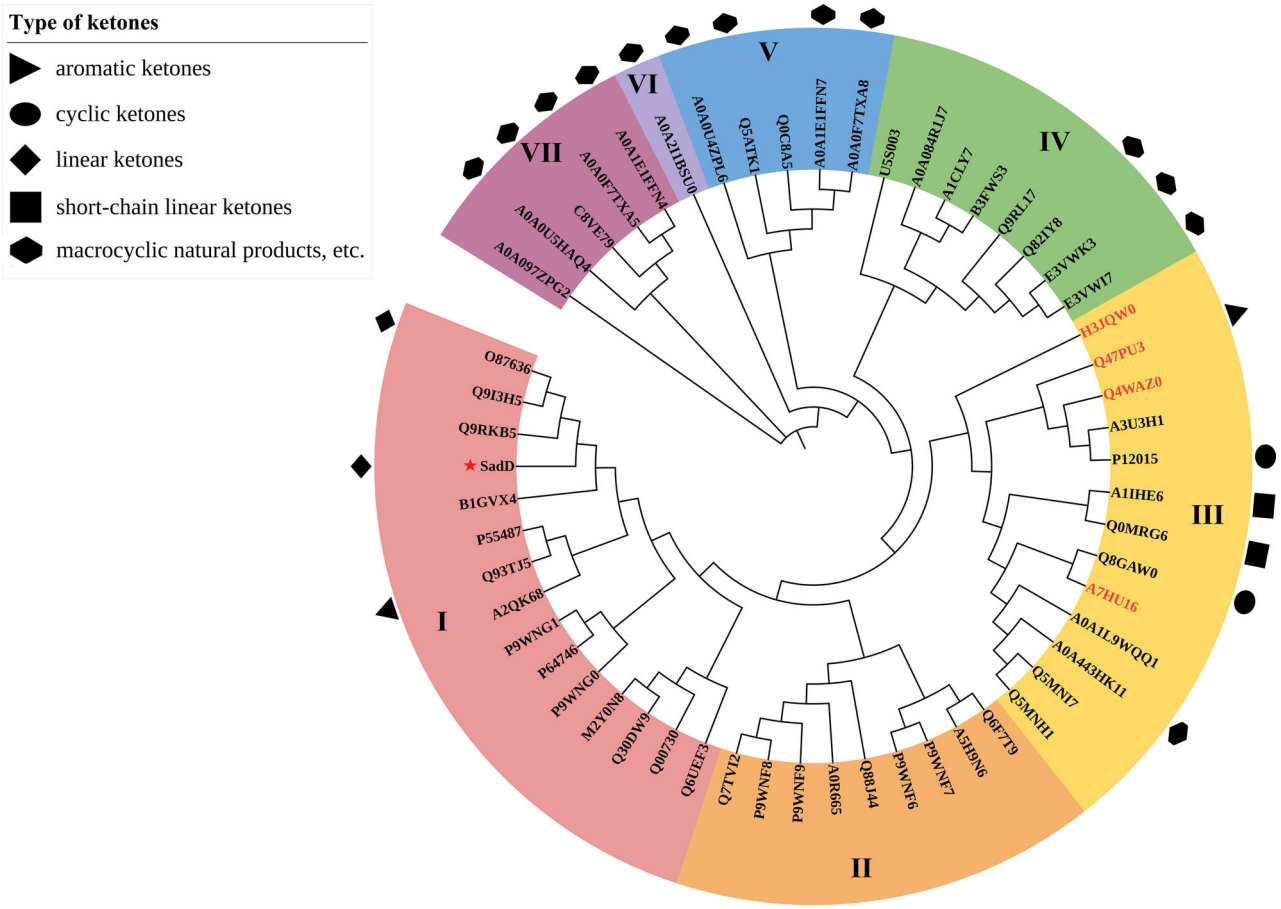

FIGURE 6 Maximum likelihood phylogenetic tree of the reviewed BVMOs and their different substrate specificities. The phylogenetic tree was constructed with bootstrap 1000 replicates using RAxML-NG (Stamatakis, 2014), and visualized by iTOL (Letunic & Bork, 2019). Seven clades were identified based on clustering. The different shapes of graphic symbols mark the type of ketones which were substrates for functionally characterized BVMOs. The proteins with red colours of UniProt entries indicate the availability of crystal structures. Protein sequences are represented with the corresponding UniProt entries. SadD in this study is indicated by a red star. BmoF1 (UniProt entry: O87636) from strain DSM 50106 (Kirschner et al., 2007b) is the only other studied protein sharing a similar substrate profile with SadD. BVMOs, Baeyer–Villiger monooxygenases

A wide coexistence of the genes encoded SadD homologues with those for prototypical alkane terminal hydroxylases AlkM (Ratajczak et al., 1998) and AlmA (Throne-Holst et al., 2007) in available bacterial genomes suggested that sub-terminal and terminal oxidation pathways served as two alternative strategies for bacterial alkane degradation in many single bacterial strains. Nevertheless, the relative importance of these two alkane-degrading pathways in bacteria remained obscure (Forney & Markovetz, 1970; Stephens & Dalton, 1986). It was reported that three propane-degrading strains belonging to the same genus of *Arthrobacter* but had different catabolic pathways (with terminal oxidation pathway only in one case or with both pathways in the other two cases) (Stephens & Dalton, 1986). Although alkanes degradation seems to occur in a bacterium with either pathway, these often coexisted two alternative pathways may enhance the microbial capacity to adapt to complex environment by improving carbon utilization efficiency or tackling different types of substrates. For example, unsaturated alkenes usually mixed with alkanes in crude oil were more readily transformed with the sub-terminal oxidation pathway (Markovetz et al., 1967). Nevertheless, it is clear that full understanding of the significance of the coexisted two pathways will require further research, particularly the characterization of the sub-terminal hydroxylases catalysing the initial degradation of alkanes.

Like certain BVMOs with distinct substrate preferences used in the field of pharmaceutical chemistry (Fürst et al., 2019), SadD characterized here is exclusively active towards aliphatic ketones. A complete understanding of their structural mechanism of substrate preference was helpful for their redesign in specific environmental and industrial applications. However, exploration of this question is particularly challenging because of the absence of complex crystal structures with their substrates. There are two hypotheses on substrates of BVMOs access to the active site based on two rare

14622920, 2022, 12, Downloaded from https://sfamjournals.onlinelibrary.wiley.com/doi/10.1111/1462-2920.16124 by Shanghai Jiao Tong University, Wiley Online Library on [19/12/2022]. See the Terms and Conditions (https://onlinelibrary.wiley.com/terms-and-conditions) on Wiley Online Library for rules of use; OA articles are governed by the applicable Creative Commons License

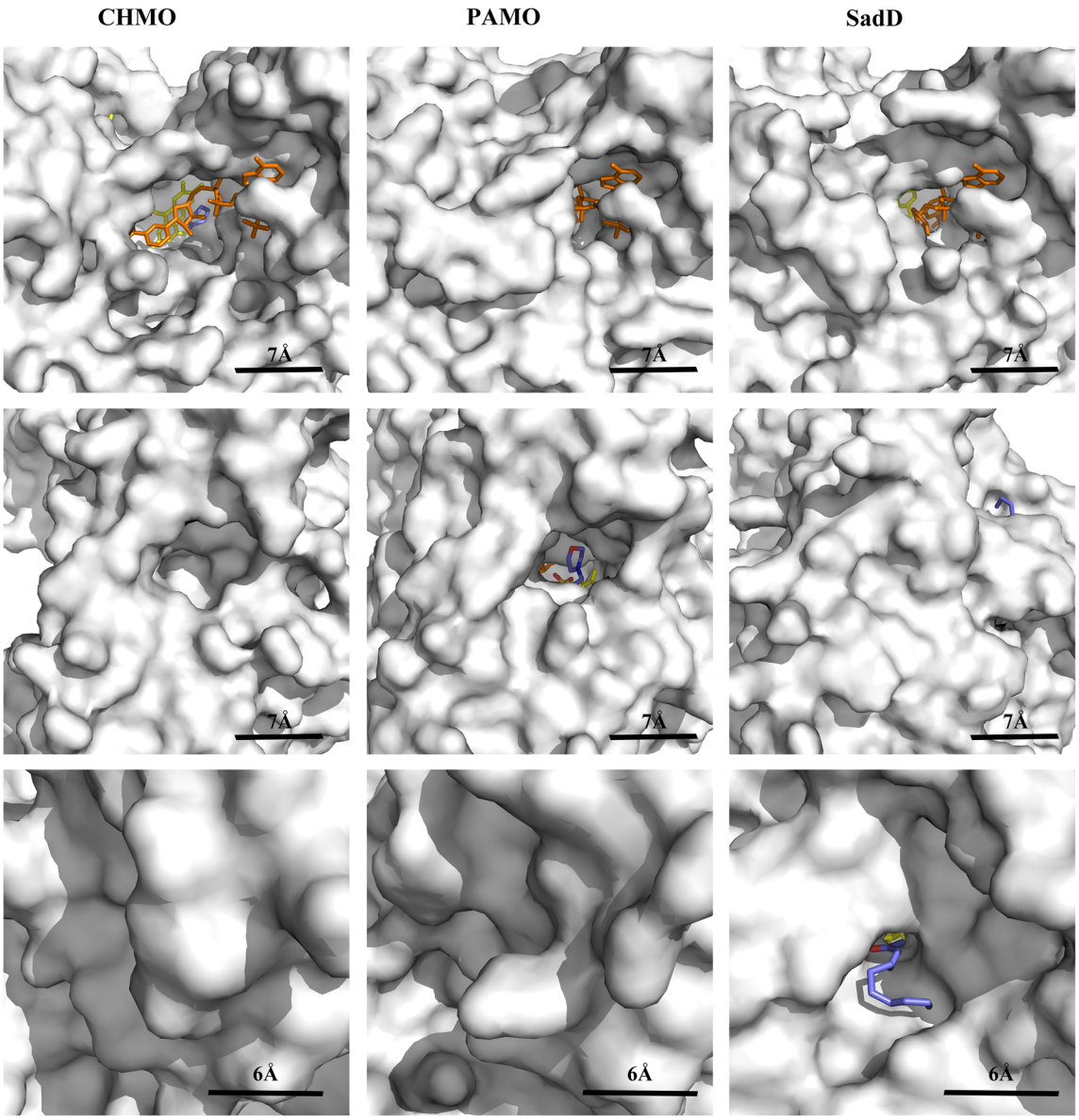

FIGURE 7 Comparison of the putative substrate channels of BVMOs among two resolved complex (CHMO and PAMO) and predicted SadD structures. CHMO (PDB ID: 3UCL) with larger pocket of $NADP^+$ makes it possible for both $NADP^+$ and substrate (cyclohexanone) entry, while the pocket of PAMO (PDB ID: 2YLT) and SadD was smaller for only $NADP^+$ access (upper panel); the tunnel of putative substrate entry [in complex with 2-(N-morpholino)-ethanesulfonic acid (MES)] at the back of $NADP^+$ pocket seen in PAMO is obstructed in CHMO and SadD (middle panel); a narrow tunnel of putative substrate entry at the back of $NADP^+$ pocket only seen in SadD which can only accommodate aliphatic substrates, the docked 2-undecanone molecule (binding energy was −4.07 kcal/mol) is oriented towards the FAD by this tunnel (lower panel). CHMO, PAMO and SadD (3D structure of SadD was predicted by AlphaFold V2.0) are shown as surface, and their ligands [$NADP^+$ in orange, FAD in yellow, carbon atoms of cyclohexanone (for CHMO), MES (for PAMO) and 2-undecanone (for SadD) in cyan] are shown as sticks. BVMOs, Baeyer–Villiger monooxygenases; CHMO, cyclohexanone monooxygenase; PAMO, phenylacetone monooxygenase

examples of complex structures bound with their substrate or inhibitor. Cyclohexanone monooxygenase (CHMO), a *chnB* gene product from *Rhodococcus* sp. HI-31 was the first BVMO whose crystal structure was resolved as a complex (PDB code: 3UCL) (Yachnin et al., 2012; Yachnin et al., 2014). This cyclohexanone-bound structure appeared the unique rotation of $NADP^+$, which indicated that CHMO may appear a series of conformational changes to gradually move the cyclohexanone from the solvent into the cyclohexanone/$NADP^+$-binding pocket observed in the complex structure. In contrast, phenylacetone monooxygenase (PAMO) (PDB ID: 2YLT), a *pamO* gene product from *Thermobifida fusca* (Orru et al., 2011), binds its weak inhibitor MES [2-(N-morpholino)-ethanesulfonic acid] in funnel-shaped cavity leading to the catalytic site, suggesting that the substrate of BVMO may also access the active sites through this separated channel. For the sake of exploring the substrate-preference mechanism of SadD in this study, we docked the 2-undecanone (binding energy:

14622920, 2022, 12, Downloaded from https://sfamjournals.onlinelibrary.wiley.com/doi/10.1111/1462-2920.16124 by Shanghai Jiao Tong University, Wiley Online Library on [19/12/2022]. See the Terms and Conditions (https://onlinelibrary.wiley.com/terms-and-conditions) on Wiley Online Library for rules of use; OA articles are governed by the applicable Creative Commons License

−4.07 kcal/mol) into protein structure of SadD predicted by AlphaFold v2.0 (Jumper et al., 2021) (Figure 7). It was found that SadD and PAMO with a narrower entry for $NADP^+$ than that of CHMO, their entries were unlikely to permit their substrates to enter after being blocked by $NADP^+$. There is a putative substrate channel in PAMO but no such channel is present in the equivalent region of the SadD or CHMO. However, another channel leading to the active sites of SadD was found, accommodating the 2-undecanone very well. This channel is long and narrow enough to only permit the access of aliphatic ketones but not for other types of ketones such as aromatic or cyclic ketones. These indicated the fact that SadD is exclusively active towards aliphatic ketones may be determined by the shape of substrate entry channel, but further prospective research is surely required for elucidating the underlying mechanisms.

ACKNOWLEDGEMENTS

This work was supported by grants from the National Key R&D Program of China (2021YFA0910300) and the National Natural Science Foundation of China (92051104).

CONFLICT OF INTEREST

The authors declare that they have no conflict of interest.

DATA AVAILABILITY STATEMENT

The genome of *Acinetobacter* sp. strain NyZ410 has been deposited in GenBank under accession number CP094620. Locus tags of *sadA*, *sadB*, *sadC* and *sadD* are MTO68_16935, MTO68_16930, MTO68_16925 and MTO68_16920.

ORCID

Chao-Fan Yin https://orcid.org/0000-0002-6905-0909
Ying Xu https://orcid.org/0000-0001-5936-0818
Tao Li https://orcid.org/0000-0002-8255-7798
Ning-Yi Zhou https://orcid.org/0000-0002-0917-5750

REFERENCES

Austin, R.N. & Groves, J.T. (2011) Alkane-oxidizing metalloenzymes in the carbon cycle. *Metallomics*, 3, 775–787.

Darriba, D., Posada, D., Kozlov, A.M., Stamatakis, A., Morel, B. & Flouri, T. (2020) ModelTest-NG: a new and scalable tool for the selection of DNA and protein evolutionary models. *Molecular Biology and Evolution*, 37, 291–294.

Dell' Anno, F., Rastelli, E., Sansone, C., Brunet, C., Ianora, A. & Dell' Anno, A. (2021) Bacteria, fungi and microalgae for the bioremediation of marine sediments contaminated by petroleum hydrocarbons in the omics era. *Microorganisms*, 9, 1695.

Dudek, H.M., Fink, M.J., Shivange, A.V., Dennig, A., Mihovilovic, M. D., Schwaneberg, U. et al. (2014) Extending the substrate scope of a Baeyer–Villiger monooxygenase by multiple-site mutagenesis. *Applied Microbiology and Biotechnology*, 98, 4009–4020.

Edgar, R.C. (2021) *MUSCLE v5 enables improved estimates of phylogenetic tree confidence by ensemble bootstrapping*. *bioRxiv*, 2021.06.20.449169.

Feng, L., Wang, W., Cheng, J., Ren, Y., Zhao, G., Gao, C. et al. (2007) Genome and proteome of long-chain alkane degrading *Geobacillus thermodenitrificans* NG80-2 isolated from a deep-subsurface oil reservoir. *Proceedings of the National Academy of Sciences of the United States of America*, 104, 5602–5607.

Finn, R.D., Clements, J. & Eddy, S.R. (2011) HMMER web server: interactive sequence similarity searching. *Nucleic Acids Research*, 39, W29–W37.

Forney, F.W. & Markovetz, A.J. (1970) Subterminal oxidation of aliphatic hydrocarbons. *Journal of Bacteriology*, 102, 281–282.

Fürst, M.J.L.J., Gran-Scheuch, A., Aalbers, F.S. & Fraaije, M.W. (2019) Baeyer–Villiger monooxygenases: tunable oxidative biocatalysts. *ACS Catalysis*, 9, 11207–11241.

Ji, Y., Mao, G., Wang, Y. & Bartlam, M. (2013) Structural insights into diversity and *n*-alkane biodegradation mechanisms of alkane hydroxylases. *Frontiers in Microbiology*, 4, 58.

Jumper, J., Evans, R., Pritzel, A., Green, T., Figurnov, M., Ronneberger, O. et al. (2021) Highly accurate protein structure prediction with AlphaFold. *Nature*, 596, 583–589.

Kiamarsi, Z., Soleimani, M., Nezami, A. & Kafi, M. (2019) Biodegradation of n-alkanes and polycyclic aromatic hydrocarbons using novel indigenous bacteria isolated from contaminated soils. *International journal of Environmental Science and Technology*, 16, 6805–6816.

Kielkopf, C.L., Bauer, W. & Urbatsch, I.L. (2020) Methods for measuring the concentrations of proteins. *Cold Spring Harbor Protocols*, 2020, 102277.

Kirschner, A., Altenbuchner, J. & Bornscheuer, U.T. (2007a) Design of a secondary alcohol degradation pathway from *Pseudomonas fluorescens* DSM 50106 in an engineered *Escherichia coli*. *Applied Microbiology and Biotechnology*, 75, 1095–1101.

Kirschner, A., Altenbuchner, J. & Bornscheuer, U.T. (2007b) Cloning, expression, and characterization of a Baeyer-Villiger monooxygenase from *Pseudomonas fluorescens* DSM 50106 in *E. coli*. *Applied Microbiology and Biotechnology*, 73, 1065–1072.

Letunic, I. & Bork, P. (2019) Interactive tree of life (iTOL) v4: recent updates and new developments. *Nucleic Acids Research*, 47, W256–W259.

Li, L., Liu, X., Yang, W., Xu, F., Wang, W., Feng, L. et al. (2008) Crystal structure of long-chain alkane monooxygenase (LadA) in complex with coenzyme FMN: unveiling the long-chain alkane hydroxylase. *Journal of Molecular Biology*, 376, 453–465.

Markovetz, A.J., Klug, M.J. & Forney, F.W. (1967) Oxidation of 1-tetradecene by *Pseudomonas aeruginosa*. *Journal of Bacteriology*, 93, 1289–1293.

Medema, M.H., Takano, E. & Breitling, R. (2013) Detecting sequence homology at the gene cluster level with MultiGeneBlast. *Molecular Biology and Evolution*, 30, 1218–1223.

Morris, G.M., Huey, R., Lindstrom, W., Sanner, M.F., Belew, R.K., Goodsell, D.S. et al. (2009) AutoDock4 and AutoDockTools4: automated docking with selective receptor flexibility. *Journal of Computational Chemistry*, 30, 2785–2791.

Nie, Y., Chi, C.Q., Fang, H., Liang, J.L., Lu, S.L., Lai, G.L. et al. (2014) Diverse alkane hydroxylase genes in microorganisms and environments. *Scientific Reports*, 4, 4968.

Orru, R., Dudek, H.M., Martinoli, C., Torres Pazmino, D.E., Royant, A., Weik, M. et al. (2011) Snapshots of enzymatic Baeyer-Villiger catalysis: oxygen activation and intermediate stabilization. *The Journal of Biological Chemistry*, 286, 29284–29291.

Ratajczak, A., Geissdorfer, W. & Hillen, W. (1998) Alkane hydroxylase from *Acinetobacter* sp. strain ADP1 is encoded by *alkM* and belongs to a new family of bacterial integral-membrane hydrocarbon hydroxylases. *Applied and Environmental Microbiology*, 64, 1175–1179.

Rojo, F. (2009) Degradation of alkanes by bacteria. *Environmental Microbiology*, 11, 2477–2490.

14622920, 2022, 12, Downloaded from https://sfamjournals.onlinelibrary.wiley.com/doi/10.1111/1462-2920.16124 by Shanghai Jiao Tong University, Wiley Online Library on [19/12/2022]. See the Terms and Conditions (https://onlinelibrary.wiley.com/terms-and-conditions) on Wiley Online Library for rules of use; OA articles are governed by the applicable Creative Commons License

Rojo, F. (2010) Enzymes for aerobic degradation of alkanes. In: *Handbook of hydrocarbon and lipid microbiology*. Berlin, Germany: Springer, pp. 781–797.

Sambrook, J., Fritsch, E.F. & Maniatis, T. (1989) *Molecular cloning: a laboratory manual (2nd ed.)*. New York, NY: Cold Spring Harbor Laboratory Press.

Schrodinger, LLC. (2015) The PyMOL Molecular Graphics System, Version 1.8.

Stamatakis, A. (2014) RAxML version 8: a tool for phylogenetic analysis and post-analysis of large phylogenies. *Bioinformatics*, 30, 1312–1313.

Stephens, G.M. & Dalton, H. (1986) The role of the terminal and subterminal oxidation pathways in propane metabolism by bacteria. *Microbiology*, 132, 2453–2462.

Throne-Holst, M., Wentzel, A., Ellingsen, T.E., Kotlar, H.K. & Zotchev, S.B. (2007) Identification of novel genes involved in long-chain n-alkane degradation by *Acinetobacter* sp. strain DSM 17874. *Applied and Environmental Microbiology*, 73, 3327–3332.

Van Beilen, J.B., Wubbolts, M.G. & Witholt, B. (1994) Genetics of alkane oxidation by *Pseudomonas oleovorans*. *Biodegradation*, 5, 161–174.

Volker, A., Kirschner, A., Bornscheuer, U.T. & Altenbuchner, J. (2008) Functional expression, purification, and characterization of the recombinant Baeyer-Villiger monooxygenase MekA from *Pseudomonas veronii* MEK700. *Applied Microbiology and Biotechnology*, 77, 1251–1260.

Wentzel, A., Ellingsen, T.E., Kotlar, H.K., Zotchev, S.B. & Throne-Holst, M. (2007) Bacterial metabolism of long-chain *n*-alkanes. *Applied Microbiology and Biotechnology*, 76, 1209–1221.

Yachnin, B.J., Sprules, T., McEvoy, M.B., Lau, P.C.K. & Berghuis, A. M. (2012) The substrate-bound crystal structure of a Baeyer–Villiger monooxygenase exhibits a Criegee-like conformation. *Journal of the American Chemical Society*, 134, 7788–7795.

Yachnin, B.J., McEvoy, M.B., Maccuish, R.J.D., Morley, K.L., Lau, P. C.K. & Berghuis, A.M. (2014) Lactone-bound structures of cyclohexanone monooxygenase provide insight into the stereochemistry of catalysis. *ACS Chemical Biology*, 9, 2843–2851.

Yang, J., Yang, Y., Wu, W.M., Zhao, J. & Jiang, L. (2014) Evidence of polyethylene biodegradation by bacterial strains from the guts of plastic-eating waxworms. *Environmental Science & Technology*, 48, 13776–13784.

How to cite this article: Yin, C.-F., Xu, Y., Li, T. & Zhou, N.-Y. (2022) Wide distribution of the *sad* gene cluster for sub-terminal oxidation in alkane utilizers. *Environmental Microbiology*, 24(12), 6307–6319. Available from: https://doi.org/10.1111/1462-2920.16124

14622920, 2022, 12, Downloaded from https://sfamjournals.onlinelibrary.wiley.com/doi/10.1111/1462-2920.16124 by Shanghai Jiao Tong University, Wiley Online Library on [19/12/2022]. See the Terms and Conditions (https://onlinelibrary.wiley.com/terms-and-conditions) on Wiley Online Library for rules of use; OA articles are governed by the applicable Creative Commons License